Runaway electron production during intense electron beam penetration in dense plasma

P. B. Parks, and T. E. Cowan

Citation: Physics of Plasmas **14**, 013102 (2007); doi: 10.1063/1.2424430
View online: https://doi.org/10.1063/1.2424430
View Table of Contents: http://aip.scitation.org/toc/php/14/1
Published by the American Institute of Physics

Runaway electron production during intense electron beam penetration in dense plasma

P. B. Parks[a)]
General Atomics, P.O. Box 85608, San Diego, California 92186-5608

T. E. Cowan
University of Nevada-Nevada Terawatt Facility, Reno, Nevada 89557-0042

(Received 8 September 2006; accepted 24 November 2006; published online 12 January 2007)

Relativistic electrons are efficiently generated when multiterawatt lasers focused to ultrahigh intensities $\gtrsim 10^{19}$ W/cm^2 illuminate the surface of dense plasma targets. A theoretical study finds that during typical picosecond pulse widths, significant amounts of Dreicer produced runaway electrons can build up due to the high axial electric field driving the neutralizing return current. An important consequence is that there will be a conversion of plasma current to runaway electron current, which is maximized at some optimum value of the beam-to-plasma density ratio $N_b = n_b/n_e$, depending on the plasma collisionality. At collisionalities representative of solid target experiments, complete conversion to runaway electrons can only take place over a certain range of N_b values. At higher collisionalities and pulse widths, applicable to the fast ignition concept for inertial confinement fusion, it was found that conversion to runaways has a peak at ~90% around $N_b \sim 0.06$. Significant lessening of target material heating by Joule current dissipation is also possible, since part of the beam energy loss is transferred through the electric field directly to the formation of energetic runaways. Implications for beam transport inhibition by the electric field are also discussed. © *2007 American Institute of Physics*. [DOI: 10.1063/1.2424430]

I. INTRODUCTION

The propagation of picosecond laser-accelerated electron beams in strongly collisional plasmas near solid density or greater is a rapidly growing research area for studying plasmas under extreme conditions and their applications[1–5] including fast ignition for inertial confinement fusion.[6–10] Numerous interaction mechanisms can arise when a high current electron beam propagates through dense collisional plasma.[11–14] When the electron beam is "switched on," the transient magnetic field associated with the rising beam current I_b causes a back emf (electromotive force) because of the Faraday induction law. As a result, a plasma return current I_p is generated in the opposite direction by the (inductive) electric field E that tends to cancel the original beam magnetic field, leaving a net current $I_{\rm net} = I_b + I_p \ll I_b$. This is what is meant by current neutralization and it is one of the essential requirements for propagation of high current electron beams in plasma without the benefit of a static magnetic guide field.[15–18] Current neutralization is temporary, however, since diffusion leads to the decay of the return current on the characteristic skin time $t_d \approx 4\pi\sigma a^2/c^2 = (a^2/\lambda^2)\tau$, where a is the radius of the beam, $\sigma = \omega_p^2 \tau/4\pi$ is the conductivity of the plasma (ω_p is the plasma frequency), $\lambda = c/\omega_p$ is the collisionless skin depth, and τ is an electron collisional relaxation time. In cold, dense plasmas, binary collision rates typically dominate over effective collisional rates stemming from collective effects such as ion acoustic turbulence. Consequently, we shall use in this paper the collisional relaxation time associated with the Spitzer conductivity,[19] $\tau = \tau_c = m^{1/2} 2(2T_e)^{3/2} \delta_z/(n_e Z e^4 \pi^{3/2} \ln \Lambda_t)$, with m the electron mass, n_e the plasma electron density, Z the effective ionic charge, and δ_z a coefficient having a weak Z dependence. The skin time is significant because the degree of current neutralization $f_m \equiv I_{\rm net}/I_b$ after a beam pulse time t_b will be $f_m \approx t_b/t_d$ (for $t_b \ll t_d$). The net current has to be less than the Alfvén current $I_A = (mc^3/e)\beta\gamma$ (γ is the relativistic Lorentz factor) in order for the beam to propagate in the first place.[15] Hence, the beam current cannot exceed a maximum value; i.e., $I_b < I_{\rm max} = I_A/f_m$. For the recent experiments with aluminum and CH target plasmas,[1–5] we take $I_b \sim 4$ MA, $t_b = 0.45$ ps, $\gamma = 2$, $a = 5$ μm, $T_e \sim 100$ eV, $n_e \sim 10^{23}$ cm^{-3}, obtaining $\tau_c \sim 3.4$ fs, $\lambda = 0.0168$ μm, $\tau_d \sim 0.3$ ns, and thus $I_{\rm max} = 23$ MA, indicating that the beam is well neutralized and therefore—in the absence of beam-plasma instabilities—should propagate intact over its entire pulse length. We only deal with stable beam propagation into a thick target, one for which target thickness d exceeds $c \cdot t_b$. Our model does not apply to thin targets, where the fast electrons would reflect off the space-charge field set up on the back surface of the target. In thin targets after a few fast electron bounce times $c \cdot t_b \gg d$, there would be no return current or inductive electric field to drive runaways. However, in the fast ignition concept,[6–10] the electron beam must carry an exceedingly high power flux $\sim 10^{19}$–10^{20} W/cm^2, and current ~100 MA, within a beam diameter of a few tens of micrometers. For nominal electrical conductivities and beam pulse lengths (1–10 ps) expected in fast ignition, the criteria $I_b < I_{\rm max}$ is very demanding, making it uncertain whether the beam can propagate over a distance of several hundreds of micrometers up to its final absorption zone.

However, if the return current were to be carried by a

a)Electronic mail: parks@fusion.gat.com

nonthermal electron component, t_d could be effectively lengthened, thus allowing for a larger $I_{\max}$ and beam current. Due to the strong (inductive) electric field that drives the return current, the Dreicer runaway electron production mechanism[20] could lead to a sizable portion of the return current carried by a suprathermal electron population. The present paper is devoted to the examination of the runaway current generation in connection with laser-generated electron beams. We will present a self-consistent solution of the runaway current alongside the evolution of the electric field responsible for their generation. The current carried by Dreicer runaways will be derived rigorously using a kinetic equation approach, which represents an improvement over simpler models that were, e.g., employed in the study of runaway currents in tokamak plasmas.[21] We will show that in existing laser-matter experiments the runaway current grows steadily during the beam pulse width; i.e., on the time scale of 0.2 to 0.5 ps. In some cases the electric field falls to zero and complete conversion of plasma return current to runaway current takes place. The key result in this paper is therefore the runaway conversion time, and its dependence on plasma and beam parameters. For the recent experiments, the model predicts a conversion time smaller than the beam pulse length, indicating that the beam current might be completely neutralized by runaways during the later part of the beam pulse time t_b.

Our model presented here is based on Maxwell's equations in a cylindrically axisymmetric system. Our equations assume a "rigid" axisymmetric beam model where the beam is to be regarded as a given "source" term in Maxwell's equations. We must, therefore, restrict ourselves to the study of beam propagation where the division of the beam and return current into a number of small filaments does not happen. The azimuthal magnetic field surrounding the beam can pinch the beam,[17] or the beam can widen. We therefore have to assume that the beam forms a stable channel already in transverse pressure balance with the magnetic field.

Accounting for beam filamentation on runaway electrons is beyond the present scope of this manuscript. The dynamics of beam filamentation and coalescence of filaments is not yet well understood. It is known from two-dimensional particle-in-cell simulations[11,14] that the process leads to an *enhanced* generation of transverse magnetic fields at the expense of beam energy. To build up the magnetic field and extract beam energy on a faster time scale than the ordinary resistive skin time scale τ_d, implies that anomalously large inductive electric fields E_z are generated. Such large fields could also enhance the runaway production rate and feed back on the dynamics of filamentation.

II. ELECTROMAGNETIC FIELD AND TIME SCALES OF THE PLASMA RESPONSE

For simplicity, we consider a uniform cylindrical beam of radius a and number density n_b immersed in an unbounded plasma. The beam is moving in the axial $+z$ direction with velocity $v \approx c$ and the axial direction is assumed to be the ignorable coordinate. At $t=0$, the beam is instantaneously switched on to full current density J_b, which persists for the duration of the beam pulse t_b. This model is tantamount to considering the propagation of a uniform blunt beam extending from $z=-\infty$ to $z=v\,t$.[11] Hence, the distance *behind* the beam front x corresponds to the time $t=x/v$. We may assume that the beam current is constant during the runaway growth period. This assumption is valid even if the beam is losing a great deal of energy by slowing down in the electric field because the change in the beam velocity is still small ($\delta v/v=\delta\gamma/\gamma^3 \ll 1$) for large beam energy: $\gamma \geqslant 2$. The beam pulse length is assumed to be much shorter than the characteristic time for the onset of motion. With immobile ions, and quasineutrality assumed, the plasma electron density n_e (and skin depth λ) may be treated as constants (valid provided $n_b \ll n_e$).

The starting point is Maxwell's equations in a axisymmetric cylindrical coordinate system (r,ϑ,z) the magnetic field takes the form $\mathbf{B}=B_\vartheta(r,t)\hat{\vartheta}$. Writing $\nabla\times\mathbf{A}=\mathbf{B}$, with magnetic flux function $\mathbf{A}=A(r,t)\hat{z}$, the scalar function A satisfies the z component of Ampère's law (neglecting displacements currents)

$$\frac{1}{r}\frac{\partial}{\partial r}\left(r\frac{\partial A}{\partial r}\right) \equiv \nabla^2 A = \frac{-4\pi}{c}(J_b + J_p + J_r), \tag{1}$$

where the plasma return current density is given by Ohm's law:

$$J_p = \sigma E - \tau_c \frac{\partial J_p}{\partial t}, \tag{2}$$

and Faraday's law $E=(-\partial A/\partial t)/c$, eliminates the axial inductive electric field. The runaway current density J_r will be specified in Sec. IV. We may dispense with the radial component of Ampère's law and neglect the electrostatic potential in Faraday's law as well. The only possible radial current comes from the plasma electrons expelled out of the beam region by the beam's space-charge field. However, it is recognized that the space-charge fields will be nullified on the fast charge neutralization time scale $\sim(4\pi\sigma)^{-1}\sim 0.01$ fs[18] (or $\omega_p^{-1}\sim 0.03$ fs, if $\omega_p\tau_c>1$). In the case of a blunt beam, charge neutralization occurs within a short distance behind the beam front $x_c=c/(4\pi\sigma)\sim 0.003\ \mu$m. Since $J_{pr}/J_p \sim E_r/E \sim x_c/a \sim 3\times 10^{-4}$ ($a\sim 10\ \mu$m), we need not consider radial fields and currents any further.

After substituting Eq. (2) into Eq. (1), and then eliminating the longitudinal electric field by using we obtain a partial differential equation for A

$$\frac{\partial A}{\partial t} = \lambda^2\nabla^2\left(\frac{1}{\tau_c}+\frac{\partial}{\partial t}\right)A + \frac{4\pi\lambda^2}{c}\left(\frac{1}{\tau_c}+\frac{\partial}{\partial t}\right)(J_b + J_r). \tag{3}$$

We suppose that the beam current is suddenly rising, such that in this initial period $\tau_c\partial/\partial t \gg 1$; i.e., the inertial impedance of the plasma electrons dominates their collisional impedance. In addition, since Dreicer produced runaways have no time to form, Eq. (3) reduces to a time-independent form

$$\nabla^2 A - \frac{A}{\lambda^2} = -\frac{4\pi}{c}J_b. \tag{4}$$

The analytic solution of this equation agrees with Hammer and Rostoker,[15] or Lee and Sudan,[22] who apply the Fourier-

Laplace transform technique to the "blunt beam" problem. The important result is the net current density inside the beam region $J_{\text{net}}=J_b+J_p$, given by

$$\frac{J_{\text{net}}}{J_b} = -\Lambda I_0(\Lambda r/a)K_1(\Lambda) \sim \left(\frac{a}{4r}\right)^{1/2} \exp[-(a-r)/\lambda]. \tag{5}$$

Usually, $\Lambda \equiv a/\lambda$ is a very large number so that the net current in the bulk of the beam region is zero except in a narrow boundary layer of width comparable to the collisionless skin depth λ. Now, on the time scale longer than the collision time, $\tau_c \partial/\partial t \ll 1$, Eq. (3) reduces to the induction equation

$$\frac{\partial A}{\partial t} - \frac{a^2}{\tau_d}\nabla^2 A = \frac{c}{\sigma}(J_b + J_r). \tag{6}$$

As we have seen, the net current is initially zero so that $\nabla^2 A \sim 0$, and later on as the current diffuses $a^2\nabla^2 \ll 1$. Therefore, the resistive diffusion term in Eq. (6) can be neglected if the time scale of interest is *shorter* than the skin time; i.e., $\tau_d \partial/\partial t \gg 1$. Note that after neglecting the resistive diffusion term, the curl of Eq. (6) becomes the same equation (with $J_r=0$) used in Refs. 16 and 17 for the study of electron beam transport in solid targets when magnetic diffusion, and thermal conduction are negligible. Consequently, Eq. (6) leads to the "zero current" condition during the runaway growth period:

$$J_b + J_r + J_p = J_{\text{net}} \approx 0, \tag{7}$$

in which $J_p \cong \sigma E$, in the limit $\tau_c \partial/\partial t \ll 1$. To summarize the above, if the runaways evolve on the time scale bounded by $\Lambda^{-2} \ll \tau_c \partial/\partial t \ll 1$, Eq. (7) holds during the runaway current evolution. We return to Eq. (7) after considering the runaway current evolution.

Before closing this section, it is necessary to mention that the entire concept of electrical conductivity and Ohm's law breaks down when the relative drift velocity u_{rel} between the electrons and the (immobile) ions exceeds roughly the electron thermal speed $v_{\text{th}}=(2T_e/m)^{1/2}$. Since $u_{\text{rel}}=N_b c$ ($N_b \equiv n_b/n_e$), our model is restricted to beam densities that satisfy $N_b < v_{\text{th}}/c$. In fast ignition, the fast electrons are created at the critical surface with a pulse width of 1–10 ps, and must propagate as a collimated beam to the high-density core and deposit their energy for spark ignition. The initial temperature of the plasma electrons near the critical surface could be 0.2–3 keV, although the temperature will increase rapidly by resistive heating, as we shall see. Therefore, we must restrict ourselves to $N_b < \sim 0.1$ in the fast ignition situation; otherwise, our results start to become unreliable for larger N_b. This restriction may not be problematic, despite the fact that all the electrons created at the critical surface can be converted to hot electrons making it seem at first sight that N_b might be greater than unity. However, the energy spectrum of fast electrons produced at n_{crit} resembles some sort of thermal distribution. The forward energy flux is carried by only a few of the most energetic electrons; i.e., those able to surmount the restraining electrostatic potential barrier due to charge imbalance. The lower energy electrons in the distribution will be reflected off the barrier and not contribute to the forward propagating beam. Hence, it is probable that $N_b \ll 1$ at, or near to, the critical surface. Certainly, a large drop in N_b occurs in a very short propagation distance away from the critical surface due to the colossal density gradient created under the action the laser light pressure.[7,12] Consideration of propagation in density gradients would have to be considered in a future study in order to better quantify the role of runaway electrons in fast ignition. At this point, we are striving for conceptual understanding rather than quantitative accuracy.

III. RUNAWAY ELECTRON PRODUCTION RATE AND KEY DEFINITIONS

Two kinds of runaway generation processes can exist simultaneously: primary or Dreicer generation,[20] and secondary or knock-on avalanche generation.[21] In this work, we will not be concerned with the latter process, because the secondary production rate is negligibly small. In Dreicer generation, electrons from the tail of the background electron population runaway when their velocity exceeds the critical velocity v_c; determined by equating the rate of *energy gain* by accelerating in the electric field E to rate of *energy loss* by collisional drag,[20]

$$eE = \nu(v)mv\big|_{v=v_c} = \frac{4\pi n_e e^4 \ln \Lambda_c}{mv_c^2}, \tag{8}$$

where $\nu(v)=4\pi n_e e^4 \ln \Lambda(v)/m^2 v^3$ is the velocity dependent electron collision frequency, and $\ln \Lambda$, is the velocity-dependent Coulomb logarithm. The Dreicer field E_c is the electric field needed to make the thermal electrons runaway, and it is defined here as[20]

$$eE_c = \nu_t m v_t \frac{\ln \Lambda_c}{\ln \Lambda_t} = \frac{4\pi n_e e^4 \ln \Lambda_c}{mv_t^2}, \tag{9}$$

In units of eV cgs, the plasma thermal speed is $v_t = (kT_e/m)^{1/2} = 4.19\times 10^7 T_e^{1/2}$, and $\nu_t \equiv \nu(v_t) = 1.093 \times 10^{-5} n_e T_e^{-3/2} \ln \Lambda_t$ is the thermal electron collision frequency, with the Coulomb logarithms for electron velocities v_t and v_c being, respectively,

$$\ln \Lambda_t = \ln \frac{2.6\times 10^{10} T_e}{n_e^{1/2}} = \ln \frac{1.478\times 10^{-5} v_t^2}{n_e^{1/2}}, \tag{10}$$

$$\ln \Lambda_c = \ln \Lambda_t + \ln \frac{v_c^2}{v_t^2} = \ln \Lambda_t + \ln \frac{E_c}{E}. \tag{11}$$

We assume an ideal plasma domain, where $\ln \Lambda_t \gg 1$. The rate of increase in runaway number density is given by[20]

$$\frac{dn_r}{dt} \equiv S_r = \nu_t n_e K \exp(-G), \tag{12}$$

where

$$G = \frac{E_c}{4E} + 4\left[\frac{\alpha E_c}{3E}\right]^{1/2}, \quad K = C\left(\frac{E_c}{E}\right)^{\alpha}, \quad C \cong 0.35,$$

$$\alpha = 3(1+Z)/16.$$

Recent Monte Carlo simulations have verified that this analytical formula is exceptionally accurate for relative electric fields within the range of interest: $0<E/E_c<\sim 0.2$.[21] It should be emphasized that if E were to exceed $\sim 0.2E_c$, the concept of an electrical resistivity breaks down.

By combining Eqs. (9) and (11), the Dreicer field satisfies the transcendental equation

$$E_c = \frac{m v_t \nu_t}{e}\left(1+\frac{\ln(E_c/E)}{\ln \Lambda_t}\right). \tag{13}$$

As a result, the T_e and E dependencies in the important ratio E_c/E become entangled. However, separability can be achieved by introducing new nondimensional variables

$$\mathcal{E}=\frac{E}{E_{c0}}, \quad \theta=\frac{T_e}{T_{e0}}, \quad \mu=\frac{\ln \Lambda_c}{\ln \Lambda_{c0}}, \tag{14}$$

where subscript "0" here and in the following represents an initial value at $t=0$. Hence,

$$\frac{E_c}{E}=\frac{E_c}{E_{c0}}\frac{E_{c0}}{E}=\frac{\mu}{\theta \mathcal{E}}, \tag{15}$$

where function $\mu(E)$ is solved for implicitly:

$$\mu = 1+\frac{\ln(\mu \mathcal{E}_0/\mathcal{E})}{\ln \Lambda_{c0}}. \tag{16}$$

Given initial values T_{e0}, E_0, all that remains is the evaluation of $\ln \Lambda_{c0}$, and E_{c0}, and thus $\mathcal{E}_0=E_0/E_{c0}$. By evaluating (13) at $t=0$, these initial values are given by

$$E_{c0}=\frac{m v_t \nu_{t0} \kappa_0}{e}, \quad \ln \Lambda_{c0}=\kappa_0 \ln \Lambda_{t0}, \tag{17}$$

where κ_0 is given by

$$\kappa_0 = 1+\frac{\ln(\bar{u}_0 \kappa_0)}{\ln \Lambda_{t0}}, \quad \bar{u}_0 \equiv \frac{m v_{t0} \nu_{t0}}{e E_0}. \tag{18}$$

Initially, $J_r=0$, so that $\sigma_0 E_0 = e c n_b$, obtaining $eE_0 = b N_b m c \nu_{t0}$, $\bar{u}_0=\beta_{t0}/(bN_b)$, and $\mathcal{E}_0=1/(\kappa_0 \bar{u}_0)$, where $N_b=n_b/n_e$, $\beta_{t0}=v_{t0}/c$, and $b\equiv 1/(\nu_{t0}\tau_{c0})=(\pi/2)^{1/2}(Z/16\delta_z)$.

It is important to mention here that the Dreicer production formula is strictly valid only for a quasistationary situation,[20] i.e., the characteristic time for collisional upscattering to the critical velocity v_c should be considerably faster than the time variations of the macroscopic variables, $\nu_t^{-1}(E_c/E)^{3/2}\partial/\partial t<1$. Choosing plasma conditions $n_e=10^{23}$ cm^{-3}, $T_{e0}=30$ eV, and $\ln \Lambda_t=2$, we get $\nu_t^{-1}=0.075$ fs. Taking again a typical value, i.e., $E/E_c=0.1$, and $(\partial/\partial t)^{-1} \sim t_r \sim t_b \sim 0.45$ ps, we see that this inequality is indeed satisfied initially, but it may become only marginally satisfied later on, since both E/E_c and v_t are decreasing with increasing runaway current and rising plasma temperature caused by Joule heating.

IV. RUNAWAY ELECTRON CURRENT

After a runaway electron is produced at the boundary v_c it will be continuously accelerated up to velocities comparable to c. For the realistic case here, in which $v_t<v_c \ll c$, we can assume that the runaways are born with practically zero momentum. Neglecting collisions with the background electrons and ions, the kinetic equation for the distribution function f of the freely accelerating runway particles takes the form

$$\frac{Df}{Dt}=\frac{\partial f}{\partial t}+\mathbf{v}\cdot\nabla f - e\left(\mathbf{E}+\frac{\mathbf{v}\times\mathbf{B}}{c}\right)\cdot\frac{\partial f}{\partial \mathbf{p}} = \delta(p_x)\delta(p_y)\delta(p_z)S_r, \tag{19}$$

where the relativistic momentum is $\mathbf{p}=m\gamma\mathbf{v}$, and the Lorentz factor is $\gamma=(1-v^2/c^2)^{-1/2}\cong(1-v_z^2/c^2)^{-1/2}$. For good current neutralization, the magnetic field $\mathbf{B}$ is essentially zero inside the beam. Neglecting longitudinal variations as well, $\partial/\partial z$ we may drop the convective term, so that Eq. (19) reduces to a simpler form:

$$\frac{Df}{Dt}=\frac{\partial f}{\partial t}+\frac{e}{c}\frac{\partial A}{\partial t}\frac{\partial f}{\partial p_z}=\delta(p_x)\delta(p_y)\delta(p_z)S_r. \tag{20}$$

The runaway number density is $n_r=\int f d^3\mathbf{p}$, and the current density is $J_r=-e\int v_z f d^3\mathbf{p}$, where $d^3\mathbf{p}=dp_x dp_y dp_z$. Next, we apply the operator $v_z d^3\mathbf{p}$ to the above equation, and introduce dimensionless quantities $\eta=-eA/mc^2$ and $\tilde{p}=p/mc$. After integration by parts on the momentum variable $\tilde{p}_z$, we obtain

$$\frac{dJ_r}{\partial t}=m^3c^4 e\frac{d\eta}{dt}\int\frac{f d\tilde{p}_z d\tilde{p}_x d\tilde{p}_y}{(1+\tilde{p}_z^2)^{3/2}}, \tag{21}$$

where f is given by integrating Eq. (20) along the characteristics orbits in phase space:

$$f(t,\tilde{p})=\int_{-\infty}^{t} S_r(t')\delta(\tilde{p}_x')\delta(\tilde{p}_r^y)\delta(\tilde{p}_z')dt'. \tag{22}$$

Employing conservation of canonical momentum, we can write the primed momentum variable in Eq. (22) as $\tilde{p}_z'\equiv\tilde{p}_z(t')=\tilde{p}_z(t)+\eta(t)-\eta(t')$, while the other components $\tilde{p}_x, \tilde{p}_y$ remain at zero. We can then insert the resulting expressing for f into Eq. (21), and exchange the order of integration between the $\tilde{p}_z$ and t variables, obtaining

$$\frac{dJ_r}{\partial t}=ec\frac{d\eta}{dt}\int_{-\infty}^{t}\frac{S_r(t')dt'}{\{1+[\eta(t)-\eta(t')]^2\}^{3/2}}. \tag{23}$$

After integration in time, we obtain the final expression for the runaway current density

$$J_r(t)=ec\int_{-\infty}^{t}\frac{[\eta(t)-\eta(t')]S_r(t')dt'}{\{1+[\eta(t)-\eta(t')]^2\}^{1/2}}. \tag{24}$$

V. RUNAWAY CURRENT AND ELECTRIC FIELD EVOLUTION

Introducing nondimensional quantities, $\tilde{t}=\nu_{t0}t$, $q=bC/(\beta_{t0}\kappa_0)^2$, the nondimensional form of the zero current relation (7) for $\tilde{t}>0$ becomes

$$\theta^{3/2}\mathcal{E}=\mathcal{E}_0-q\beta_{t0}\kappa_0\int_0^{\tilde{t}}\frac{(\eta-\eta')\mu'^{\alpha}\exp\left[-(\mu'/4\theta'\mathcal{E}')-4(\alpha\mu'/3\theta'\mathcal{E}')^{1/2}\right]d\tilde{t}'}{\left[1+(\eta-\eta')^2\right]^{1/2}\mathcal{E}'^{\alpha}\theta'^{(\alpha+3/2)}},\tag{25}$$

where the weakly varying logarithmic term $\ln(\Lambda_t)$ was taken as constant. This integral equation must be solved together with the nondimensional form of Faraday's law $d\eta/d\tilde{t}=\beta_{t0}\kappa_0\mathcal{E}$, and an energy equation describing the evolution of the plasma temperature variable θ. The Joule heating rate $J_p\cdot E=\sigma E^2$ acts on the thermal population. Perhaps the simplest loss processes are radiation, expansion cooling, and perpendicular heat diffusion. Expansion cooling can be neglected because of our assumption of a stationary plasma; significant motion occurs on the ion sound time[25] $a/(kT_e/m_i)^{1/2}\sim 30$ ps, which is considerably longer than typical beam-pulse lengths, $<1-10$ ps. Similarly, the characteristic time scale for heat diffusion is quite long, and may be neglected as well. Let the plasma internal energy per unit plasma mass be U, then the general definition of the specific heat capacity at constant volume (no expansion) is $c_V=(\partial U/\partial T)$. Consequently, the dimensionless electron energy equation can be written as

$$\bar{c}\frac{d\theta}{d\tilde{t}}=\frac{\kappa_0\mathcal{E}^2\theta^{3/2}}{b},\tag{26}$$

where $\bar{c}=c_V/m_i$. We now have four equations for the dependent variables, $\mathcal{E}$, η, θ, and μ. Instead of using $\mathcal{E}$, it will be more convenient to define a new dependent variable representing the magnitude of the dimensionless *plasma current* $j=\theta^{3/2}\mathcal{E}$. In addition, the integral equation becomes much more manageable by letting the dimensionless magnetic flux function η be the *independent* variable and $j(\eta)$, $\theta(\eta)$, $\mu(\eta)$, and $\tilde{t}(\eta)$ the required *dependent* functions. Note that because the sign of $\mathcal{E}$ stays positive for $\tilde{t}>0$, then $\eta>0$ as well. Consequently, the coupled set of integrodifferential equations to be solved in the domain $\eta>0$ is

$$j=j(0)-q\int_0^{\eta}\frac{(\eta-\eta')\mu'^{\alpha}\theta'^{\alpha/2}\exp\left[-(\mu'\theta'^{1/2}/4j')-4(\alpha\mu'\theta'^{1/2}/3j')^{1/2}\right]d\eta'}{j'^{(\alpha+1)}\left[1+(\eta-\eta')^2\right]^{1/2}},\tag{27}$$

$$\frac{d\tilde{t}}{d\eta}=\frac{\theta^{3/2}}{\beta_{t0}\kappa_0 j},\tag{28}$$

$$\frac{d\theta}{d\eta}=Aj,\tag{29}$$

$$\frac{d\mu}{d\eta}=\frac{-\mu}{(\mu\ln\Lambda_{c0}-1)}\frac{d}{d\eta}[\ln j-(3/2)\ln\theta],\tag{30}$$

where $A=\kappa_0/(\bar{c}b\beta_{t0})$, and initial conditions are $j(0)=\mathcal{E}_0$, $\tilde{t}(0)=0$, $\theta(0)=1$, and $\mu(0)=1$. We solved this set using the method of successive approximations. Zero-order approximate solutions were sought by first differentiating Eq. (27) with respect to η, obtaining the exact result

$$\frac{dj}{d\eta}=-q\int_0^{\eta}\frac{\mu'^{\alpha}\theta'^{\alpha/2}\exp\left[-(\mu'\theta'^{1/2}/4j')-4(\alpha\mu'\theta'^{1/2}/3j')^{1/2}\right]d\eta'}{j'^{(\alpha+1)}\left[1+(\eta-\eta')^2\right]^{3/2}}.\tag{31}$$

Unlike in Eq. (27), the integral in Eq. (31) allows the approximation $(\eta-\eta')^2 \approx \eta^2$, particularly since the dominant exponential term contributes to the integral for the most part when η' is small; i.e., for $\eta' \ll \eta$. This allows us to convert Eq. (31) to an approximate second-order differential equation

$$\frac{d}{d\eta}\left[(1+\eta^2)^{3/2}\frac{dj}{d\eta}\right] + \frac{q\mu^{\alpha}\theta^{\alpha/2}\exp[-(\mu\theta^{1/2}/4j)-4(\alpha\mu\theta^{1/2}/3j)^{1/2}]}{j^{(\alpha+1)}} = 0. \tag{32}$$

Equation (32), with the additional initial condition $dj/d\eta = 0$, is then solved together with Eqs. (28)–(30) to obtain zero-order solutions of all variables. These variables are then substituted into the right-hand side of Eqs. (27) to obtain the first-order solution for j, which is then used in Eqs. (28)–(30) to obtain the first-order solutions of the other three quantities, and so on. Convergence to the true solution was obtained after only a few iterations; typically, no more than two or three are necessary for good accuracy.

VI. RESULTS AND DISCUSSION

Using the numerical scheme of the previous section, solutions of the normalized runaway current $J_r/J_b = 1 - j/j(0)$ are presented here for two cases: (I) ultrashort-pulse laser-generated hot electron bursts in solid density targets such as aluminum and plastic (CH)[1–5] and (II) nominal fast ignition conditions where a relativistic electron beam pulse propagates into a precompressed DT fuel target.[6–10]

First, we will discuss the validity of using the Spitzer conductivity model for the solid targets. The Spitzer conductivity is rigorously valid only for fully ionized, nondegenerate, and weakly coupled plasmas (low density, high temperature). In solid metals, such as aluminum, there are various conductivity models in the literature. Perhaps the most well known of these is the Lee and More (L-M) model[26] based on the Boltzmann relaxation time approximation. Perrot and Dharma-wardana[27] constructed a more sophisticated model based on density functional theory. For temperatures above ~10 eV, which is of interest to us, both models agree fairly well, i.e., within a factor of 2. In Fig. 3(b) of the Lee and More paper, the conductivity model for solid aluminum is compared with the Spitzer formula. There is, at most, only a factor-of-2 deviation of the Spitzer formula from the L-M model for $T_e > \sim 10-20$ eV. For insulators like CH (plastic) targets, the situation is more complex. The major difference occurs in the early phase where rapid phase transition from insulator to conductor occurs. Unlike conductors, there are no rigorous theoretical models describing the conductivity of insulators before the material is ionized. This is because changes in the conductivity at low temperatures are largely due to changes the effective ionization Z, which is zero initially. There is however a published heuristic model used by Batanni *et al.*,[20] but it requires knowledge of the Z evolution. Effects of electron-beam impact ionization, and field ionization and thermal heating all contribute to the initial ionization breakdown. These processes taken together are complicated by the fact that the beam may not even propagate in the assumed forward direction without first breaking down and ionizing the target. However, after subsequent heating of the material up to up to a few tens of eV the conductivity rises dramatically up to the Spitzer value where differences between insulator and metal conductivities become negligible: at ~40 eV both material have an electrical conductivity of $\sim 10^6$ mho/m, equivalent to that of nichrome, a fairly resistive alloy used in heating elements. The early time breakdown phase in insulators is therefore ignored in this model, being assumed instantaneous. Furthermore, the early transient period from room temperature up to 36 eV is probably not too important to treat since the runaways would have had no time to form, especially for metals with very high room temperature conductivity. Since we do not consider the details of the material heating below 36 eV in our Case I simulations we can justify the use of the Spitzer formula without incurring significant error.

For each case, then, we choose the following set of fixed parameters:

Case I:

$$T_{e0} = 36.1 \text{ eV}, \quad Z = 2, \quad b = 0.229, \quad \bar{c} = 3,$$

$$n_i = 10^{23} \text{ cm}^{-3}, \quad n_e = Zn_i, \quad \ln \Lambda_{t0} = 3,$$

$$\nu_{t0} = 3.027 \times 10^{16} \text{ s}^{-1}.$$

Case II:

$$T_{e0} = 200 \text{ eV}, \quad Z = 1, \quad b = 0.1346, \quad \bar{c} = 3,$$

$$n_i = 6 \times 10^{25} \text{ cm}^{-3}, \quad n_e = Zn_i, \quad \ln \Lambda_{t0} = 5,$$

$$\nu_{t0} = 1.16 \times 10^{18} \text{ s}^{-1}.$$

Since $\ln \Lambda_t$ increases very slowly with increasing temperature in the target medium due to Joule heating, we consider it to be a constant in our model. Therefore, in the above cases we set $\ln \Lambda_{t0}$ equal to some average value of $\ln \Lambda_t$ during the beam pulse. To shed light on the physical mechanisms at play, we examine the influence of normalized beam density N_b on the time-asymptotic value of the runaway current J_r/J_b. For Case I, complete conversion of the plasma current to runaway current $(J_r/J_b \to 1)$ is possible only if N_b lies within the domain $0.008\,75 \leqslant N_b \leqslant 0.06$. This so-called "plateau band" is illustrated in Fig. 1, where we see that J_r/J_b decreases monotonically from unity outside the band. In Fig. 2 we plot the time t_{80} for the runaway current to reach 80% of its asymptotic value within the plateau band. There exists a fairly broad dip in the curve, with an absolute minimum of $t_{80} = 0.418$ ps occurring at $N_b = 0.018$. Since $t_{80} < t_b \sim 0.45$ ps, the present model suggests that runaway generation is highly plausible in current experiments, and the runaway current can reach a significant fraction of the return current over the beam pulse width t_b. The temporal behaviors of the runaway current J_r/J_b, normalized plasma temperature θ, and normalized electric field $E/E_0 = \mathcal{E}/\mathcal{E}_0$, are illustrated in Figs. 3(a)–3(d), corresponding to: (a) $N_b = 0.007$, (b) $N_b = 0.018$, and (c)–(d) $N_b = 0.08$. Again, we see that the most rapid growth of runaway current occurs when N_b lies within

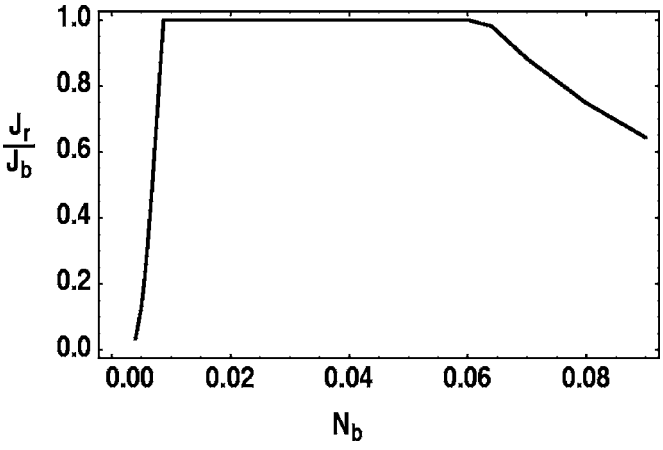

FIG. 1. Asymptotic value of the normalized runaway current density J_r/J_b as a function of normalized beam density N_b, for Case I parameters. Complete conversion of plasma return current to runaway current ($J_r/J_b=1$) is possible in the plateau band: $0.008\,75 < N_b < 0.06$.

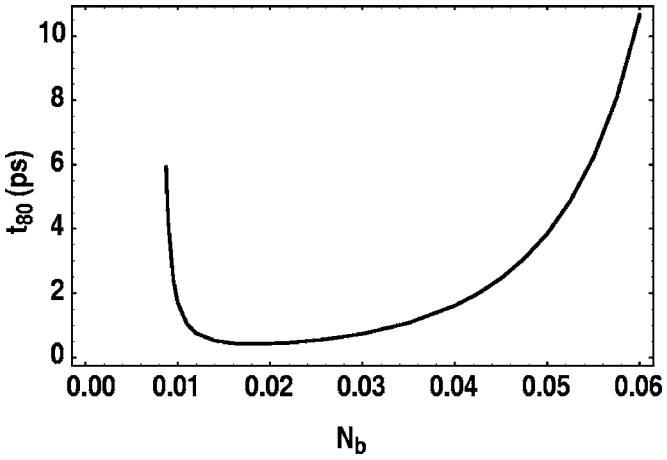

FIG. 2. Time for runaway current to reach 80% of its full value ($J_r/J_b=0.8$) when N_b lies in the plateau band, for Case I parameters.

the plateau band, Fig. 3(b). The reason for this behavior can be understood by observing the evolution of the plasma temperature due to Joule heating. Dividing Eq. (28) by (29), one recovers the nondimensional energy equation

$$\frac{d\theta^{5/2}}{d\tilde{t}} = \frac{5}{2}\kappa_0\beta_{t0}Aj^2. \tag{33}$$

At $t=0$, $\kappa_0\beta_{t0}Aj^2 \to \kappa_0\beta_{t0}A\mathcal{E}_0^2 \propto N_b^2$, so that the temperature rise by Joule heating increases with beam density (return current density), as expected. On the other hand, the initial runaway growth rate also increases rapidly with N_b, because the initial nondimensional electric field scales like $\mathcal{E}_0 \propto N_b/\kappa_0$, which has a slightly greater than linear dependence on N_b. Thus, when N_b lies outside the plateau band on the low side, as in Fig. 3(a), the runaway current generated is small, resulting in asymptotic saturation of J_r/J_b below unity; i.e., incomplete conversion results. The residual plasma current $J_p/J_b=j/j(0)$, however, continues to heat the target. Hence, the temperature rise, although small at first, is unlimited, as shown in the figure. Cessation of runaway production is caused by the electric field $\mathcal{E}=j/\theta^{3/2}$ being driven to zero by the temperature rise. When N_b lies within the plateau band the runaway growth rate is so fast that complete conversion results. In that instance, the opposite situation occurs; namely, the electric field is driven to zero because $j \to 0$, while θ is saturating asymptotically (to ~700 eV), as shown in Fig. 3(b). Ultimately, as N_b continues to increase, the competition between the temperature increase and the runaway production caused by the higher initial electric field is won by the temperature increase, which explains why asymptotic saturation of J_r/J_b below unity occurs for high N_b, as shown in Fig. 3(c), where N_b lies outside the plateau band on the high side of it. Figure 3(d) is a magnified version at early times. Note the precipitous fall in the electric field by a factor of ~30 in the first 1 fs. The runaway current J_r/J_b at that moment is hardly significant, indicating that Joule heating (rapid θ increase) is chiefly responsible for driving the electric field to zero, thus curtailing the runaway growth rate early on.

In Case II, complete conversion is not possible for any value of N_b. Instead of forming a plateau-like structure, the J_r/J_b curve assumes a local maximum of 0.884 at $N_b=0.06$, as shown in Fig. 4. The physical explanation for the peak in J_r/J_b boils down to essentially the same reason for plateau formation in Case I; namely, plasma heating tends to work against runaway electron production. To amplify this theme, we artificially reduced the temperature rise by systematically lowering the parameter A by some fractional amount, which in turn led to an increase in J_r/J_b for all values of N_b. Formation of a plateau band, as in Case I, was even possible, depending on how much A was lowered. The temporal approach of the runaway current to the asymptotic value is displayed in Fig. 5 for different values of N_b. We see that it takes only about 1 to 2 ps for the runaway current to saturate. This time is smaller than or comparable to the 1–10 ps beam pulse widths projected for nominal fast ignition scenarios.

The above results have shown that runaway production can potentially allow current neutralization for a longer time, thereby allowing for propagation of ultrahigh beam currents. The final question to be asked is whether runaway production causes an appreciable reduction in the electric field, which tends to inhibit beam penetration.[16–18,23] Part of the work done by the beam electrons on the E-field goes into dissipative processes $Q=Q_p+Q_r$; i.e., Joule heating energy Q_p and runaway electron energy Q_r, and the remainder goes into building up the magnetic field (inductive) energy W_m associated with the rising I_{net} (decaying I_p). By invoking Poynting's theorem, Lovelace and Sudan[24] deduced the general relation, $W_m/Q=f_m^2/(2f_m-f_m^2)$. Thus, when the beam current is highly neutralized, i.e., $f_m \ll 1$, $W_m/Q \sim f_m/2$ irrespective of the plasma conductivity (or the amount of runaways produced). In that case essentially all of the kinetic energy lost by the electron beam goes into dissipative processes Q. The rate of beam particle energy loss, neglecting collisional stopping,[18] is given by $mc^2 d\gamma/dt=-ev_bE \cong -ecE$. This can be integrated to obtain the (negative) change in the dimensionless kinetic energy of the beam $\Delta\gamma$ in terms of the nondimensional magnetic flux function,

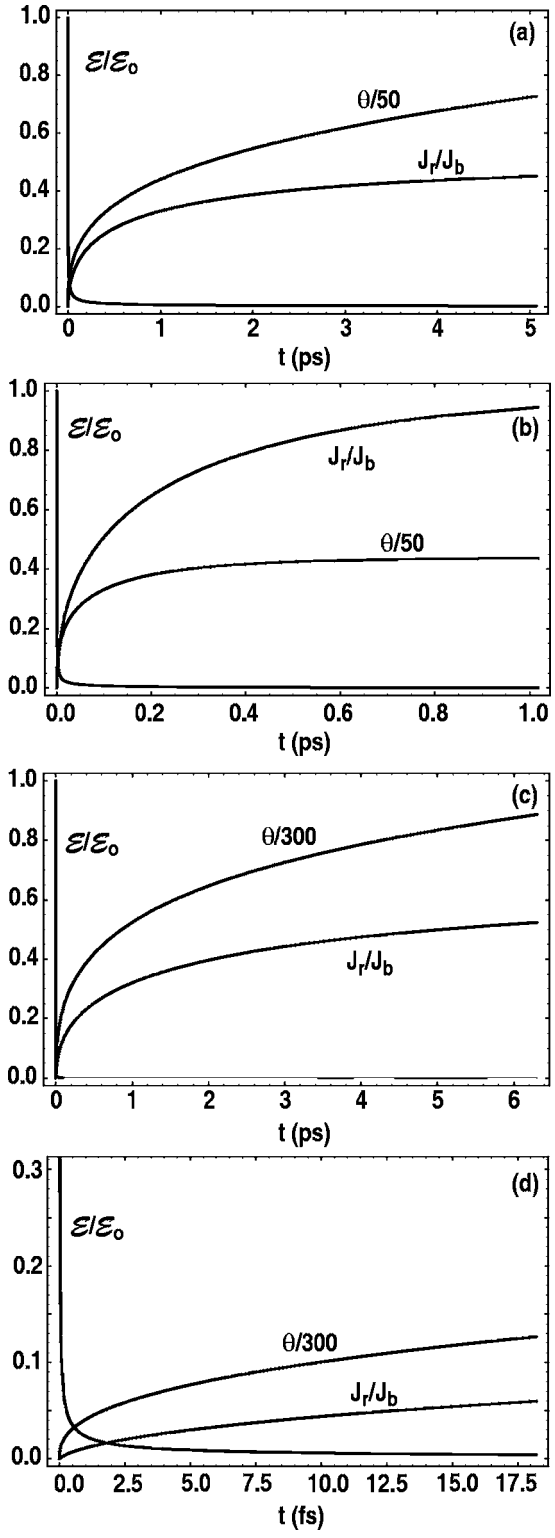

FIG. 3. The temporal behaviors of the normalized runaway current J_r/J_b, normalized plasma temperature θ, and normalized electric field $E/E_0 = \mathcal{E}/\mathcal{E}_0$, corresponding to: (a) $N_b=0.007$; (b) $N_b=0.018$; (c)–(d) $N_b=0.08$, for Case I parameters.

$$\Delta\gamma = -\eta(t) \quad \text{(with runaways)}. \tag{34}$$

Now, if we arbitrarily force the runaway current to be zero, so that $j \to j(0)=E_0$, and $\eta(t) \to \eta_{nr}(t)$, the beam energy change in the absence of runaways would be

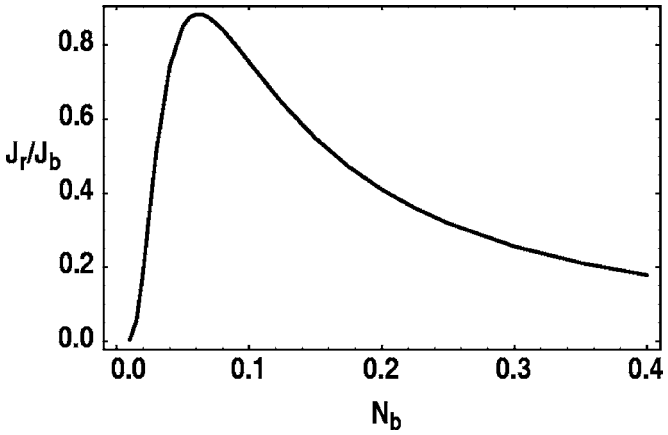

FIG. 4. Asymptotic value of the normalized runaway current density J_r/J_b as a function of normalized beam density N_b for Case II parameters.

$$\Delta\gamma = -\eta_{nr}(t) \quad \text{(no runaways)}, \tag{35}$$

where $\eta_{\rm nr}(t)$ can be found analytically by solving Eqs. (28) and (33) together, obtaining

$$\eta_{\rm nr} = \frac{\bar{c}\beta_{t0}^2}{N_b}\left[\left(1+\frac{5bN_b^2\nu_{t0}t}{2\bar{c}\beta_{t0}^2}\right)^{2/5}-1\right]. \tag{36}$$

Note in the limit that N_b becomes very small, Eq. (36) shows that $\eta_{nr} \sim N_b$, and thus electric field inhibition of beam transport is not significant for low beam densities. In Figs. 6 we have compared the two curves $\eta(t)$ (solid curve) and $\eta_{\rm nr}(t)$ (dashed curve) for the Case I parameters using the same beam densities corresponding to Fig. 3. We see that beam energy loss $\Delta\gamma$ can be sizably reduced by runaway generation only if N_b lies in the plateau band [see Fig. 3(b)]. For all beam densities in Case I the relative energy loss $\Delta\gamma/(\gamma-1)$ due to the electric field force is still fairly modest if $\gamma>3-4$. This is not so for the fast ignition Case II. For example, taking $t_b=4$ ps, we find that the values for $\eta(t_b)$ corresponding to the beam densities $N_b=0.025$, 0.06, and 0.2 are $\eta(t_b)=11$, 9.22, and 7.32, respectively. Notice how the initial target collisionality ν_{t0} enters into Eq. (36), which explains why the magnitudes of $\eta(t_b)$ and thus $-\Delta\gamma$ are so much larger for the fast ignition Case II compared to Case I. This result

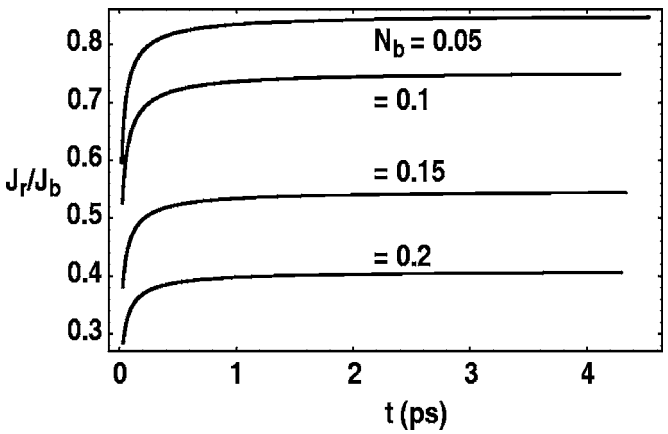

FIG. 5. Evolution of normalized runaway current J_r/J_b for Case II parameters, and different values of normalized beam density N_b.

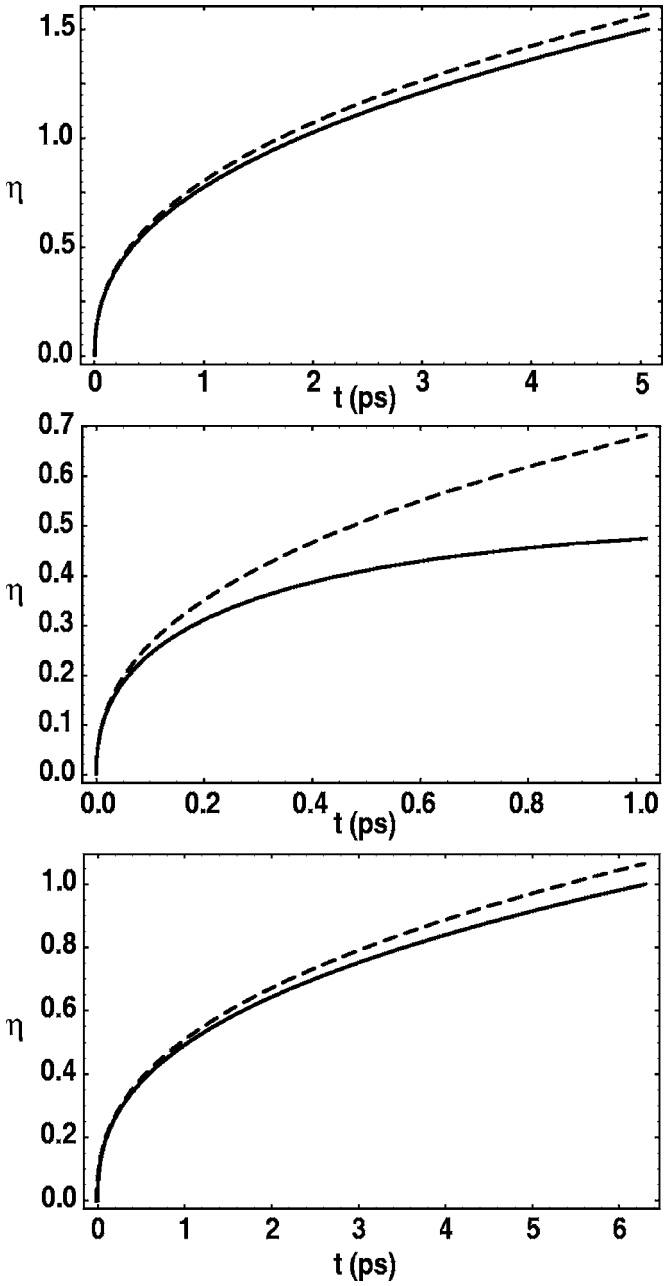

FIG. 6. Illustrates the reduction in the temporal growth of the dimensionless magnetic flux function $\eta=\beta_{i0}\kappa_0\int \mathcal{E}d\tilde{t}$ when runaway electrons are included (solid curve). Case I parameters are used here. For comparison, the dashed curve corresponds to the case where runaway electrons are deliberately turned off.

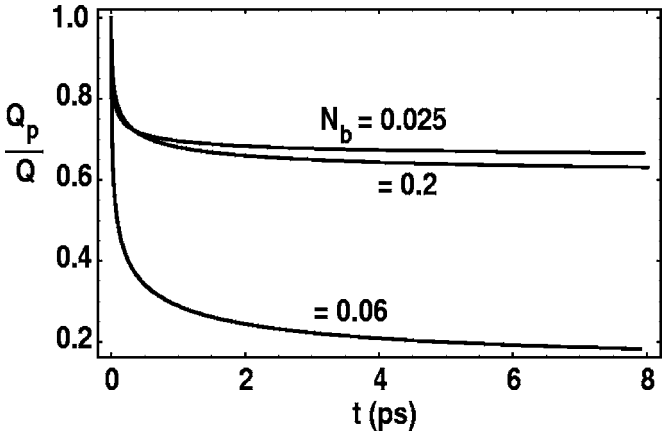

FIG. 7. Fraction of beam energy lost Q dissipated in Joule heating the target plasma Q_p versus time for different beam densities N_b in Case II.

indicates that strong beam stopping will occur in fast ignition unless the average energy of the beam electrons is well above 10 MeV, in agreement with Refs. 16 and 17. We also found that the $\eta(t)$ and $\eta_{\rm nr}(t)$ curves are only slightly different from each other for any value of N_b. [No plot is shown, since Eq. (36) becomes a good approximation for $\eta(t)$.]

From this result, and Figs. 6(a) and 6(b) of Case I, it might be inferred that runaway electron generation has very little effect on the electric field *whenever there is only partial runaway conversion*. This appears to be due to the fact that a *partial* reduction in plasma return current j leads to reduced Joule heating, and thus temperature θ, leaving $\mathcal{E}=j/\theta^{3/2}$ relatively unchanged.

Although in Case II the formation of runaway electrons has little effect on the amount of beam energy loss, it can significantly affect how this energy loss is partitioned into the Joule heating the target plasma and runaway electron acceleration. The fraction of beam energy loss Q converted to Joule heating Q_p is given by

$$\frac{Q_p}{Q}=\frac{\int J_p\cdot Edt}{\int J_b\cdot Edt}=\frac{\int_0^\eta \frac{j(\eta')}{j(0)}d\eta'}{\eta}. \tag{37}$$

This result was evaluated and is plotted verses time for three different beam densities, N_b=0.025, 0.06, and 0.2 (see Fig. 7). Clearly, when the conversion to runaway electron current is highest, as it is for N_b=0.06, (see Fig. 4) the fraction Q_p/Q is lowest ~20%. Consequently, this study predicts that almost 80% of beam energy loss can be converted to runaway electron energy for laser pulse times greater than ~4 ps, which is a typical pulse width for fast ignition.

In conclusion, the electric field will inhibit penetration of fast-electron beams emanating from the laser spot in fast ignition targets to values well below the expected collisional range.[17] Heating of the compressed target core can be significantly reduced, however, when large quantities of runaway electrons are produced and accelerated to high energies during the beam pulse.

ACKNOWLEDGMENTS

Work supported by the U.S. Department of Energy under DE-FC02-04ER54698 and DOE/NNSA under UNR grant DE-FC08-01NV14050.

[1] F. N. Beg, A. R. Bell, A. E. Dangor *et al.*, Phys. Plasmas **4**, 447 (1997).
[2] J. Fuchs, T. E. Cowan, P. Audebert *et al.*, Phys. Rev. Lett. **91**, 255002 (2003).
[3] T. E. Cowan, J. Fuchs, H. Ruhl *et al.*, Phys. Rev. Lett. **92**, 204801 (2004).
[4] P. A. Norreys, K. M. Krushelnic, and M. Zepf, Plasma Phys. Controlled Fusion **46**, B13 (2004).
[5] C. Ren, M. Tzoufras, F. S. Tsung *et al.*, Phys. Rev. Lett. **93**, 185004

(2004).
[6]M. H. Key, Nature (London) **412**, 776 (2001).
[7]R. Kodama, P. A. Norreys, K. Mima *et al.*, Nature (London) **412**, 798 (2001).
[8]O. Willi, Philos. Trans. R. Soc. London, Ser. A **357**, 555 (1999).
[9]A. I. Mahdy, H. Takabe, and K. Mima, Nucl. Fusion **39**, 467 (1999).
[10]K. A. Tanaka, R. Kodama, Y. Kitagawa, K. Kondo, and K. Mima, Plasma Phys. Controlled Fusion **46**, B41 (2004).
[11]M. Honda, J. Meyer-ter-Vehn, and A. Pukhov, Phys. Rev. Lett. **85**, 2128 (2000).
[12]Y. Sentoku, K. Mima, Z. M. Sheng, P. Kaw, K. Nishihara, and K. Nishikawa, Phys. Rev. E **65**, 046408 (2002).
[13]F. Califano, F. Pegoraro, and S. V. Bulanov, Phys. Rev. E **56**, 963 (1997).
[14]T. Taguchi, T. M. Antonsen, C. S. Liu, and K. Mima, Phys. Rev. Lett. **86**, 5055 (2001).
[15]D. A. Hammer and N. Rostoker, Phys. Fluids **13**, 1831 (1970).
[16]J. R. Davies, A. R. Bell, M. G. Haines, and S. M. Guerin, Phys. Rev. E **56**, 7193 (1997).
[17]A. R. Bell and R. J. Kingham, Phys. Rev. Lett. **91**, 035003 (2003).
[18]E. E. Fill, Phys. Plasmas **8**, 1441 (2001).
[19]L. Spitzer, *Physics of Fully Ionized Gases* (Interscience, New York, 1962).
[20]A. V. Gurevich and Ya. S. Dimant, Nucl. Fusion **18**, 629 (1978).
[21]L.-G. Eriksson, P. Helander, F. Andersson, D. Anderson, and M. Lisak, Phys. Rev. Lett. **92**, 205004 (2004); L.-G. Eriksson and P. Helander, Comput. Phys. Commun. **154**, 175 (2003).
[22]R. Lee and R. N. Sudan, Phys. Fluids **14**, 1213 (1971).
[23]D. Batani, J. R. Davies, A. Bernardinello *et al.*, Phys. Rev. E **61**, 5725 (2000).
[24]R. V. Lovelace and R. N. Sudan, Phys. Rev. Lett. **27**, 1256 (1971).
[25]L. C. Steinhauer and H. G. Ahlstrom, Phys. Fluids **14**, 81 (1971).
[26]Y. T. Lee and R. M. More, Phys. Fluids **27**, 1273 (1984).
[27]F. Perrot and M. W. C. Dharma-wardana, Phys. Rev. A **36**, 238 (1987).